DELPHI Collaboration

DELPHI 98-13 CAL 138
9 February, 1998

Performance of the VSAT detector at LEP II

S. Almehed, H.Carling, Ch. Jarlskog, G. Jarlskog, P. Jonsson
U. Mjörnmark, A. Nygren and N. Zimine[1]
University of Lund
G.Rinaudo and P. P. Trapani
University of Torino
P. Negri
University of Milano

Abstract

The Very Small Angle Tagger in the DELPHI experiment consists of four small calorimeter modules placed 7.7 m from the interaction point, forming two independent diagonals, designed to measure the elastic scattering of electrons and positrons (Bhabha scattering). The coverage of each module for particles of beam energy is 5 to 6.5 mrad in polar angle with an azimuthal coverage of 90 degrees. During LEP100 VSAT contributed to the luminosity measurements made by DELPHI, due to the high statistics Bhabha sample that could be recorded. It was also used to monitor the beam off-momentum background, and to provide electron tags for selecting two-photon collisions. At the higher energy and luminosity of LEP200 the selection of two-photon collisions by double tagging electrons and positrons is particularly interesting. Therefore the polar angle range will be enhanced by the installation of a new section of elliptical beampipe at the VSAT with a smaller horizontal radius to improve the acceptance of the VSAT. This takes place in the shutdown 97/98. In this report the performance of the VSAT is presented, after seven years of operation, and the precision of energy and position measurements at the higher energy of LEP200 have been evaluated.

[1]also JINR, DUBNA

1 Introduction

The VSAT detector is described in ref [1]. Four compact electromagnetic calorimeter modules were constructed using 2 r.l. tungsten absorbers with 11 interspaced silicon planes of 48x48 mm^2 area for the sampling of the longitudinal electromagnetic shower. The measurement of the shower position in the plane of the beams (x) is made using two silicon strip planes, put at the longitudinal depths of 5 and 9 r.l., and by one orthogonal strip plane (y) put a 7 r.l. depth. The instrumented acceptance of the x-planes is 48x32 mm^2. The strips are 1 mm wide. All silicon planes are 300 micron thick (made by Micron Semiconductor).

The modules are placed at an elliptical section of the beampipe located behind the superconducting quadrupoles at 7.7 m distance from the centre of DELPHI. The beampipe up till now had a horizontal inner radius of 60 mm and a vertical radius of 80 mm. The first strip measuring the x-position is about 64 mm from the beam. Figure 1 illustrate the position of VSAT in DELPHI, and figure 2 the layout of the VSAT calorimeter module.

The full area detector planes (FAD) and the strip planes obviously have different capacitance, and different frontend preamplifiers. The FADs use a LABEN 5243 preamplifier while the strips use the MSP16 surface mounted preamplifier. All preamplifiers can be fed by a test pulse to verify their operation (TESTIN). The amplifiers have a spread in rise time. TESTIN signals give rise times varying between 85 and 160 ns. The FAD preamplifier came in two batches which had rather different characteristics. One type has a linear relation with the pulse height of the test pulse, while the other saturates at large pulse heights (figure 3) The signals are also amplified on the multiplexor (MUX) card by an AD846 operational amplifier after which the rise times vary typically from 400 to 800 ns for beam generated signals.

The summed signals from the central FAD planes are used to identify events, normally a trigger threshold of 20 GeV is applied. A track-and-hold system is used; hold is delivered at a fixed time in relation to the Beam Cross Over (BCO).

The fact that the rise times were different and the hold was fixed in time was not considered to be a problem at first since LEP was commissioned using only four bunches of electrons, giving a comfortable time interval of 22 microseconds between collisions. In order to improve the LEP luminosity a so called Pretzel scheme was introduced in 1994, allowing for 8 equally spaced bunches in LEP with the still comfortable separation of 11 microseconds. However for the run in 1995 LEP switched to another scheme of bunches, thought to be better suited to future operation at high energy, which involved going back to four main bunches, but introducing up to four minibunches within the main bunch with the fairly small separation in time of 247 ns. This was a major change as regards the operation of the VSAT since the rise time of the pulses from the preamplifiers typically was more than twice this separation time, hence there were difficulties in correctly assigning the minibunches. Quite a bit of new logic had to be added in a new FASTBUS controller card called LURFB, which would be able to separate the minibunches and to issue hold signals which were displaced in time accordingly. Due to the different rise times in the modules the exact timing of the trigger gate became very critical, and one could not entirely avoid having misidentified minibunches which later had to be corrected for ([2]-[4]).

The LURFB card could only be tested and finally debugged with beam which led to a loss of the early runs in 1995, notably the prescan. By the middle of August 1995 the readout was stable and we got most of the scan correctly recorded. Later, for LEP200, the LEP operations group found out that the scheme with four minibunches was not optimal and most of the running has actually been done with either a single bunch, or with only two minibunches. The minibunch separation was increased to 335 ns which made it easier for the VSAT to assign minibunch number, hence to deliver a correctly timed hold signal.

Most of the frontend electronics has remained as described in [1]. The new card, LURFB, is described below in chapter 2 as it has not previously been documented. Some more recent minor modifications to the electronics are also mentioned. In chapter 3 the performance of the VSAT during 1997, i.e. for high energy operation, is reported. The accuracy of energy measurements and position reconstruction, both important for the kinematical analysis of double tagged two photon collision, are evaluated in chapter 4. Chapter 5 describes the backgrund conditions during 1997.

2 The VSAT bunch train electronics

When the minibunch scheme was introduced in 1995 minimal changes were made to the pre-1995 electronics. All new features required to handle the new data flow was placed on a FASTBUS card LURFB (Lund University Risc FastBus). The detailed features of this card are described in [5].

The new electronics card provides a series of gating signals. If the sum of the FAD planes exceeds a trigger threshold, within a gate, a hold signal is generated at the expected peak position of the signals from the silicon planes. If there is no trigger a hold is nevertheless generated after the last minibunch. The number of the minibunch which was triggering is stored for use in the on/offline software.

One should not confuse this internal trigger information with the VSAT trigger given to DELPHI which does not consider the minibunch structure but takes the bunchtrain as a single bunch. That trigger is placed on the Local Trigger Supervisor card.

The LURFB card provides basically three different features:

- A fixed time after the BCO, the WNG1 signal from PANDORA enables the gate generator. If positive a hold is generated as described above. When the hold is sent, the current minibunch number is stored in a status register as well as the current status of the trigger threshold lines. One can accept at most eight minibunches (3 bits).

- A 20MHz FADC system records the signal representing the sum of the FAD planes. The 8-bit FADC starts sampling the summed signal at WNG1 and continues during 1.2 microseconds.

- A CPU based on the TMS320C50 Digital Signal Processor performs the formatting of the data, writing it into a Frontend Buffer, a 32k 16 bit Dual Port Memory, monitors and controls the system. The Dual Port Memory is also used to download the processor program via FASTBUS. There are programmable registers for the bunch interspace time, and number of minibunches. There are also registers for the delays between hold to FAD and hold to strips. A separate hold is generated for each VSAT module and sent to the MUX cards.

The original frontend electronics has not changed much during seven years of operation. One modification was made in 1996; the FAD summing circuits on the MUX cards were changed to better handle large pulses, and to more exactly follow the shape of the incoming signals. The new summing circuit was found to work satisfactory.

3 Performance of the VSAT during 1997

Before datataking the amplification of the FAD and strip planes in all modules are roughly equalized using the TESTIN signal by adjusting a potentiometer on the MUX card. At the end of the year, before dismounting the VSAT, another check is made, the result of which, for 1997, is shown in figure 4. One observes that none of the channels is dead, but that a few channels have significantly larger or smaller response, something that, in principle, can be dealt with offline by adjusting calibration constants. The low response of FAD3 in module B1 appeared during the last week of 1997 data taking. One should note that sofar the shower position is calculated from the information in the x1 plane only, where the acceptance in x is about 16 strips (all working very well), and from the y planes, where events are concentrated at the centre, with very few entries close to the very edge where the strips seems not well adjusted.

In 1997 LEP has been running at three different energies: a calibration run at the Z peak (45 GeV beams), a run to verify preliminary data of ALEPH where four-jet events reconstructed to a peak at 130-136 GeV (65-68 GeV beams), and high energy running using 91 GeV beams. These different conditions allowed us to compare the Bhabha signals from the VSAT over a large energy range.

Figure 5 shows the relative response of the 11 FAD planes at 45 and 68 GeV of the four modules for the Bhabha peak. The modules B2 and F2 are placed on the outside of the LEP ring, while B1 and F1 are on the inside. B refers to backward and F to forward, i.e. the directions of positrons and electrons respectively. The distributions look quite acceptable. However when comparing 45 and 91 GeV, figure 6, an unpleasant feature appears: the FAD planes 3 to 5, at shower maximum, 6 to 10 r.l. deep, show severe "saturation" effects in modules B1, B2 and F2. This implies that the energy is not correctly measured. As discussed below in more detail, this is caused by the failure of the frontend amplifiers to give the same rise time for large signals as for small signals, hence the hold is coming on the rising edge for large signals, resulting in a compression of all signals above a certain magnitude. In principle a later hold would be required, but moving the hold to later times would cause misidentification of minibunches.

In principle it is possible to decrease the amplification of the FAD amplifiers so that the outputs at 91 GeV saturate less (but then the full dynamic range of the 8-bit ADC is not explored). Such adjustments were done already after 1996 where the same saturation effects were observed for some channels at the beam energy of 80 GeV. As an alternative way to avoid this problem in the 1996 and 1997 data we therefore investigated if the signals from the strip planes, which are put around shower maximum, at 5, 7 and 9 r.l. depth, could be used to replace the saturating FAD planes.

The strips have been equalized in response using bhabha events. Figures 7 and 8 illustrate that the two x-planes and the y-plane all have quite nice uniformity.

The energy depositions for the three strip planes are illustrated in figures 9 and 10 where the strip with the maximum signal has been placed at the centre. One observes that most of the energy to a good approximation is delivered to the three central strips. Summing the signals in those three strips, and use these instead of FAD 3-5, the energy measurement over the acceptance of the strip plane appears uniform, see figs 11 and 12, except for the y-plane where no energy correction was made for shower leakage in the vertical direction (this can of course be done). Figure 13 illustrate the longitudinal deposition of energy at 45 and 91 GeV in the four modules, where the strip planes have been added at positions 3, 5 and 7. The saturating FAD planes are located at positions 4, 6 and 8. The plot at 45 GeV shows that the energy spread in the strip planes is about the same as in the FAD planes. The calibration of the summed strips relative the FAD planes, is done by adjusting them to the shower profile at 45 GeV. At 91 GeV is there a fraction of events where the strip signal overflows the ADC (figure 8).

The conclusion is that one can use the energy deposition in the strip planes to improve the overall energy measurement. This can best be done on data summary tapes (DST) but requires that the strip information is kept - sofar the calculation of the position is made in the DELANA processing, based on a fit to the strip with maximum energy deposition and the two neighbouring strips, and the information of the actual signal levels of the individual strips are not put on DST. This has now been modified so that the three strips around maximum are kept in each modules.

The FADC information from the LURFB has been used in two way. Firstly, the timing of the gate for the trigger must be set so that minibunches are correctly assigned. A study was made for the case of LEP using two minibunches. In the beginning of 1997, during the Z-calibration run, the WNG1 time delay of 5.60 microseconds, relative BCO, was used. Figure 14 illustrates that in three of the modules a minibunch two event was often labelled as minibunch one. It is the large summed signals which are misidentified. The timing was then adjusted to 5.55 microseconds delay and a similar plot in figure 15 at 68 GeV shows that there are very few misidentifications. The time interval between samples is 50 ns. Part of the FADC information is passed on to DST, namely the value at the trigger threshold, and at the next FADC sample. This can be used to identify misidentifications offline. Events tagged as minibunch 2 or misidentified are not used in this analysis.

Secondly the FADC information is used to study the performance of the amplifiers as a function of pulse height. In a special study only one FAD plane was selected to form the "sum" used in the trigger, and recorded by the FADC. It is then crucial that the summing circuit is fast enough to follow the incoming signal; as mentioned above a new fast summing circuit was installed 1996. This study show that the rise times vary significantly between individual FAD planes, and that the signals at shower maximum tend to saturate. Figure 16 illustrates this. On the horizontal axis is the pulse height, and on the vertical axis the time for the pulse to reach its maximum. The latest observed peak time is in B2 FAD 3 which reaches the peak 650 ns after WNG1, while the fastest gets there after only 300 ns. One also observes another effect, namely that the peaking time depends on the pulse height. The pulse shapes from the FADC, from which e.g. figure 16 was derived, are shown in figure 17. The fact that the amplifiers fail to give the same rise time over the full dynamic range is one cause of the observed "saturation". What happens is that when the rise time is rather slow the hold is delivered on the still rising signal, i.e. before the peak, where all large pulses are compressed to the maximum value allowed by the too slow amplifier.

Ideally one would of course have liked to use different frontend electronics, but the problems reported are by no means fatal. One cure is, as mentioned above, to decrease the amplification for the FADs 3-5 where saturation is observed, and another cure is to include the strip planes in the energy reconstruction.

4 The accuracy of position and energy reconstruction from 1997 data

Since both strip planes in x work well, i.e. x1 and x2, one can compare the difference in the reconstructed x-positions. Fig. 18 shows such a comparison at 45 GeV and 91 GeV. The mean is not centered exactly at zero, reflecting the mean angle of impact of the Bhabha electrons (the longitudinal separation between the two planes is 26 mm). The width of the distribution is around 270 microns at 45 GeV, implying an error in the position reconstruction of 190 microns. At 91 GeV the mean values of the differences x1-x2 are about the same, but the widths are more narrow with a sigma of 190 microns, indicating a position resolution in each plane of 135 microns. This assumes no correlations in the reconstruction. Due to the similarity of the planes there could be a bias of reconstruction, e.g. towards the centres of the 1 mm wide strips. But the overall x- and y-distributions at 91 GeV, shown in figure 19, are rather smooth and do not reflect the pitch of the strips in any significant way. The conclusion of this study is that one ought to use the x2-plane as well to improve the position reconstruction. The position resolution scales roughly as the inverse of the square root of the energy, as expected from statistics.

In order to investigate the possible nonlinearity of the energy measurement due to saturating FAD planes a study was first performed on whether the strip planes could substitute the FADs at shower maximum. During 1997 the LEP energies were 45.6, 65.1, 68.1 and 91.5 GeV. The VSAT took data with two different time delays for the hold, so the comparison is done separately for those two settings, 5.60 and 5.55 microseconds. All 45.6 GeV data were taken with the first setting while the other energies used the second setting. A special run was taken at 91.5 GeV with the same condition as for 45.6 GeV. About 10000 Bhabha events were selected at each energy.

The Bhabha pair was required to be colinear in x and y with an impact more than 3 strips away from the inner edge (to reduce leakage corrections). Figure 20 shows the colinearity of the diagonal modules in the Bhabha sample. Pedestals were calculated for each energy and the offline calibration constants were used. There is no correction applied to the sum of the three nearby strips used for the energy measurement (some of the energy is delivered outside those three strips), and due to overflowing strip ADC. It has been checked that applying these corrections do not, within errors, change the results.

The background reduction used to remove accidental bhabhas is to require a colinear bhabha. It is possible statistically to remove the background energy spectra using the single electron trigger. This is not done in this analysis. The results are not sensitive, within errors, to the method used to remove the background.

Table 1 gives the (arbitrary) pulse height of the four modules and their ratio at 91.5/45.6 where the strip planes have replaced the three saturated FAD planes in each module. The one standard deviation error of the energy measurement is also given. The errors are purely statistical. The modules are quite uniform. In Table 2 the energies 65.1, 68.1 and 91.0 are compared using the more recent setting for the hold. One observes that the energy seen by the VSAT is slightly higher at the nominal 91.0 GeV, in all four modules. Again the modules are rather uniform in response although the forward modules F1 and F2 tend to indicate a higher energy at 91 GeV.

Tables 3 and 4 show the same conditions but now using the FAD planes as usual. The saturation effect lowers the response at high energy somewhat, as expected, except for module F1 where almost no saturation was at hand. Table 5 show how well one can estimate the electron energy for two-photon physics at high energy running. The Bhabha peak at 91 GeV is used to calibrate the module. At 65 GeV the module would give an energy of 64 GeV, and at 45.6 GeV the module would say 44 GeV. Figures 21 and 22 shows the energy response versus the beam energy. The energy scale is set by the 91.0 GeV point, and it is assumed that the calibration constants are not different between the two timings of the HOLD.

In future DELANA reprocessing the strip information will be transmitted to DST allowing the strip planes to be included in the energy reconstruction of the modules.

5 Background monitoring

The VSAT modules are also used for online monitoring of beam background. The rates of offmomentum electrons hitting the modules are recorded in BKGRD2. The single electron rates, normalized to the Bhabha rates, for our 20 GeV threshold is shown in fig. 23. At 45 GeV the relative background rate is 20, at 65 GeV about 30, while the conditions at high energy are more noisy with single electron rates typically 100 times the Bhabha rate, and with a relatively large spread during the fill. One notices that conditions improved towards the end of 1997 when a new optics was introduced, i.e. there was a change from 90/60 to 102/90. The background energy spectra at 91 GeV are shown in figure 24. Figure 25 gives a general impression of background conditions for the Bhabha trigger in the four modules. The online measurements are not in any noticable way affected by the saturation effects observed.

6 Conclusions

The VSAT modules, after seven years of operation in DELPHI, very close to the beam, are still performing well. The electronics has some limitation in dynamic range, and in handling the minibunch scheme of LEP. The quality of position reconstruction is already excellent and can be improved further using the information also from the second x-plane, sofar only used as a backup. An accuracy around 150 microns is possible to achieve at 91 GeV. The operational amplifiers used for the full area silicon detectors are a bit slow and not very uniform resulting in a certain nonlinearity in the energy measurement. Normalizing the response of the modules to the Bhabha peak at 91 Gev, using the three strip planes instead of the three Full Area silicon Detector planes at the peak of the shower, the energy measured would deviate by about three percent from the nominal value at 45 GeV, if no correction is applied.

References

[1] S. Almehed et al, NIM A305 (1991) 320-330

[2] Ch. Jarlskog, VSAT energy calibration for 1995 minibunch data, LUNFD6/(NFFL-7129)/1996

[3] Ch. Jarlskog, Energy measurement in 1995 scan data with the VSAT, LUNFD6/(NFFL-7153)/1998 (to be published)

[4] Ch. Jarlskog, VSAT offline minibunch tagging for the 1995 scan, LUNFD6/(NFFL-7154)/1998 (to be published)

[5] The Vsat bunch train scheme, H. Carling et al, Lund University 1996 (not published)

Energy	45.6	91.5
ratio	1.00	2.007
peak B1	387.5±0.4	793.9±0.6
ratio	1.00	2.049±0.003
sigma/peak (%)	5.23±0.12	4.05±0.11
peak B2	411.5±0.8	835.2±1.1
ratio	1.00	2.030±0.005
sigma/peak (%)	5.85±0.19	5.13±0.26
peak F1	367.0±0.5	770.6±0.7
ratio	1.00	2.100±0.003
sigma/peak (%)	5.92±0.16	4.30±0.14
peak F2	439.9±0.6	910.5±1.0
ratio	1.00	2.070±0.004
sigma/peak (%)	5.84±0.21	4.19±0.17

Table 1: Comparison between different energies at the timing of WNG1=5.60 microsec. FAD 3,4, and 5 replaced with strip planes

Energy	65.1	68.1	91.0
ratio	1.00	1.046	1.398
peak B1	559.7±0.4	585.1±0.4	792.2±0.5
ratio	1.00	1.045±0.001	1.415±0.001
sigma/peak (%)	4.73±0.10	4.70±0.11	3.97±0.09
peak B2	590.2±0.4	617.6±0.6	833.3±0.6
ratio	1.00	1.046±0.001	1.412±0.002
sigma/peak (%)	4.88±0.14	4.71±0.14	4.66±0.11
peak F1	532.8±0.4	560.5±0.4	761.7±0.5
ratio	1.00	1.052±0.001	1.430±0.001
sigma/peak (%)	5.06±0.13	4.77±0.09	4.33±0.08
peak F2	635.1±0.6	666.8±0.6	904.1±0.7
ratio	1.00	1.050±0.001	1.424±0.002
sigma/peak (%)	4.90±0.17	5.00±0.20	4.24±0.09

Table 2: Comparison between different energies at the timing of WNG1=5.55 microsec. FAD 3,4, and 5 replaced with strip planes

Energy	45.6	91.5
ratio	1.00	2.007
peak B1	395.4±0.4	772.7±0.6
ratio	1.00	1.954±0.003
sigma/peak (%)	5.12±0.12	4.23±0.12
peak B2	413.7±0.5	829.4±0.7
ratio	1.00	2.011±0.003
sigma/peak (%)	5.58±0.17	4.18±0.14
peak F1	372.2±0.4	776.8±0.6
ratio	1.00	2.087±0.003
sigma/peak (%)	5.41±0.13	3.89±0.11
peak F2	443.6±0.4	878.8±1.00
ratio	1.00	1.981±0.003
sigma/peak (%)	5.17±0.16	4.52±0.20

Table 3: Comparison between different energies at the timing of WNG1=5.60 microsec. FAD 3,4, and 5 are not replaced with strip planes

Energy	65.1	68.1	91.0
ratio	1.00	1.046	1.398
peak B1	578.1±0.4	603.3±0.4	790.5±0.5
ratio	1.00	1.044±0.001	1.367±0.001
sigma/peak (%)	4.50±0.10	4.34±0.10	4.30±0.08
peak B2	613.7±0.5	642.1±0.5	841.2±0.5
ratio	1.00	1.046±0.001	1.371±0.001
sigma/peak (%)	4.70±0.13	4.48±0.14	4.20±0.08
peak F1	552.5±0.4	578.7±0.4	779.5±0.6
ratio	1.00	1.047±0.001	1.411±0.001
sigma/peak (%)	4.60±0.11	4.54±0.12	4.14±0.11
peak F2	649.0±0.6	679.0±1.1	895.2±0.9
ratio	1.00	1.046±0.002	1.379±0.002
sigma/peak (%)	4.75±0.15	4.59±0.19	4.38±0.12

Table 4: Comparison between different energies at the timing of WNG1=5.55 microsec. FAD 3,4, and 5 are not replaced with strip planes

Energy (GeV)	45.6	65.1	68.1	91.0
strips B1	44.41±0.05	64.30±0.06	67.22±0.07	91.0
fads	45.63±0.06	66.55±0.06	69.45±0.06	91.0
strips B2	44.83±0.09	64.45±0.07	67.44±0.08	91.0
fads	45.15±0.06	66.39±0.07	69.46±0.06	91.0
strips F1	43.34±0.06	63.66±0.07	66.96±0.07	91.0
fads	42.99±0.06	64.49±0.07	67.55±0.07	91.0
strips F2	43.97±0.07	63.93±0.08	67.12±0.08	91.0
fads	45.55±0.07	65.97±0.09	69.02±0.13	91.0

Table 5: Reconstructed energies at 45.6,65.1, 68.1, and 91.0 GeV, normalised to 91 GeV, using strips instead af FAD 3,4,5, or only FADs

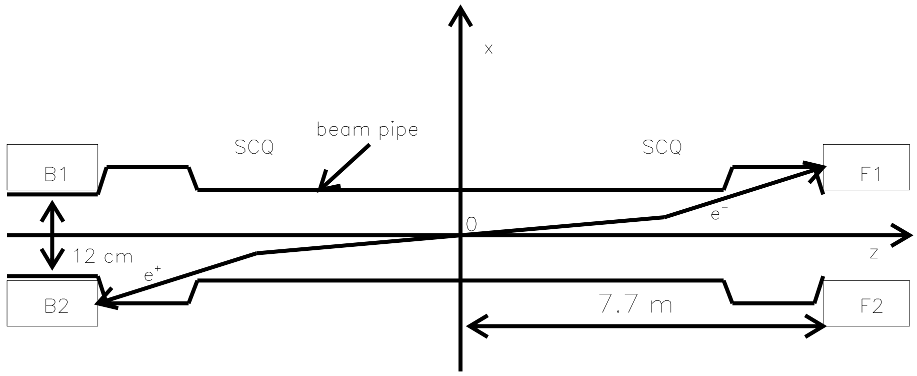

Figure 1: The position of the VSAT modules, showing the divergent effect of the quadropoles (SCQ) in the x-z plane

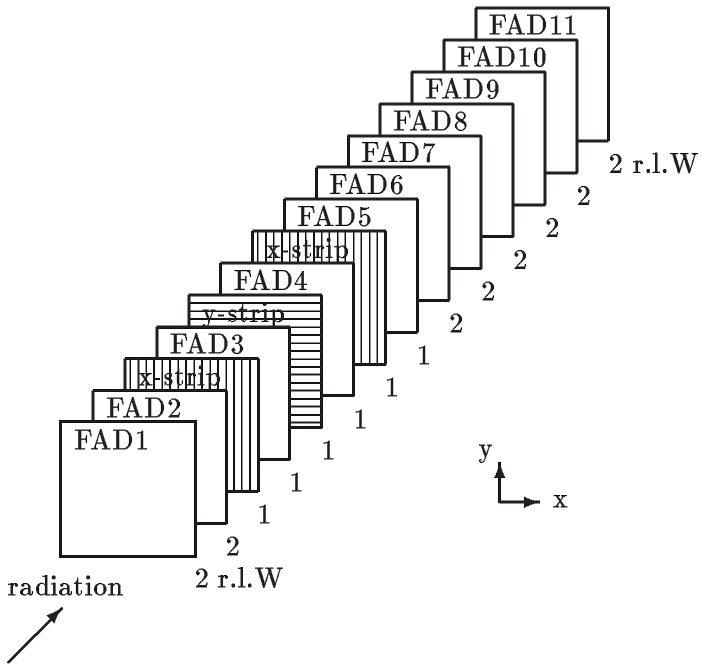

Figure 2: One of the VSAT detector modules in cross section, showing the FAD and strip planes

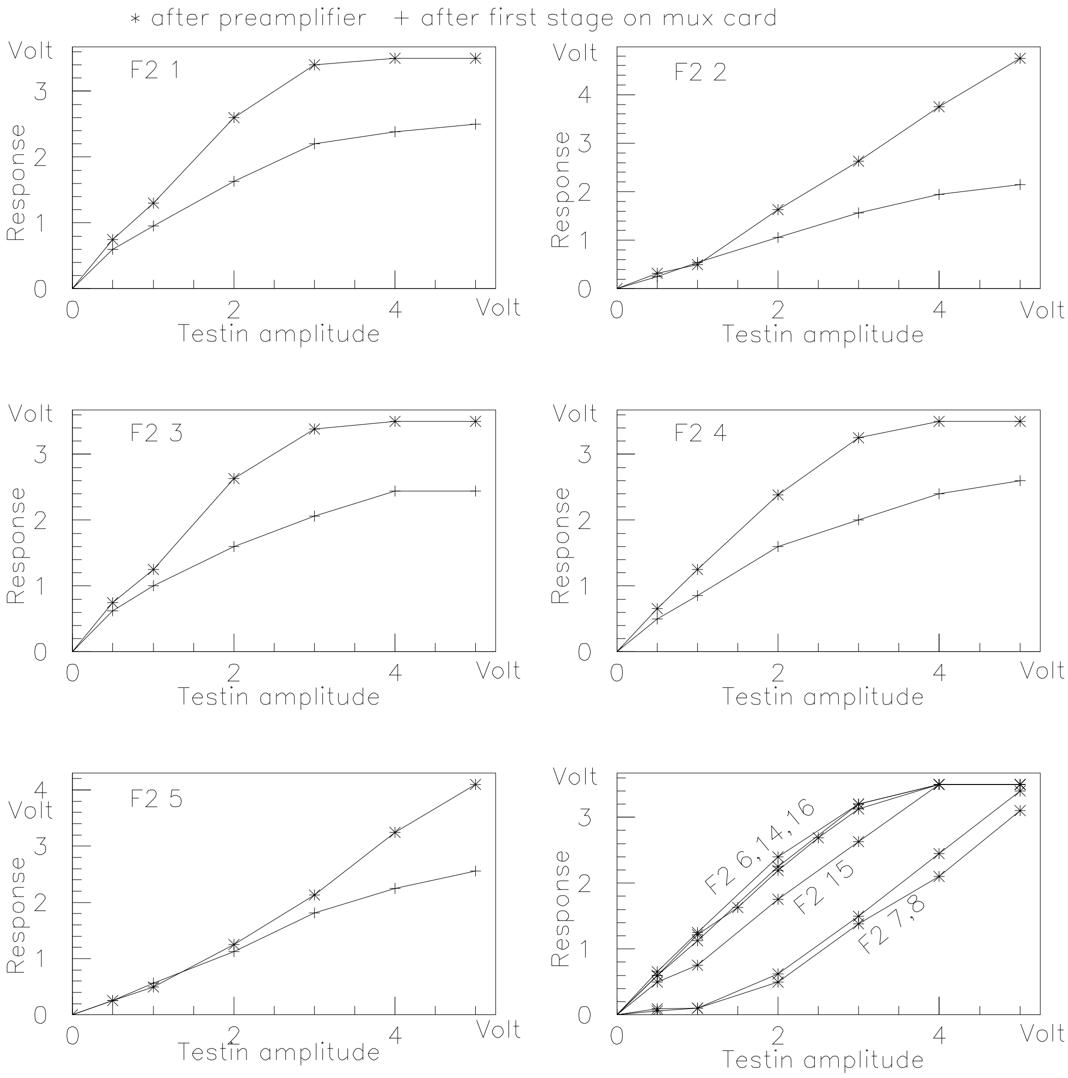

Figure 3: FAD amplifier response to TESTIN signal for module F2. For channels 1-5 is the response after the preamplifier (*) and after first amplification stage on the muxcard (+) shown. For the other channels was only the response after the preamplifier measured. The response after the preamplifier is multiplied by ten in the figure.

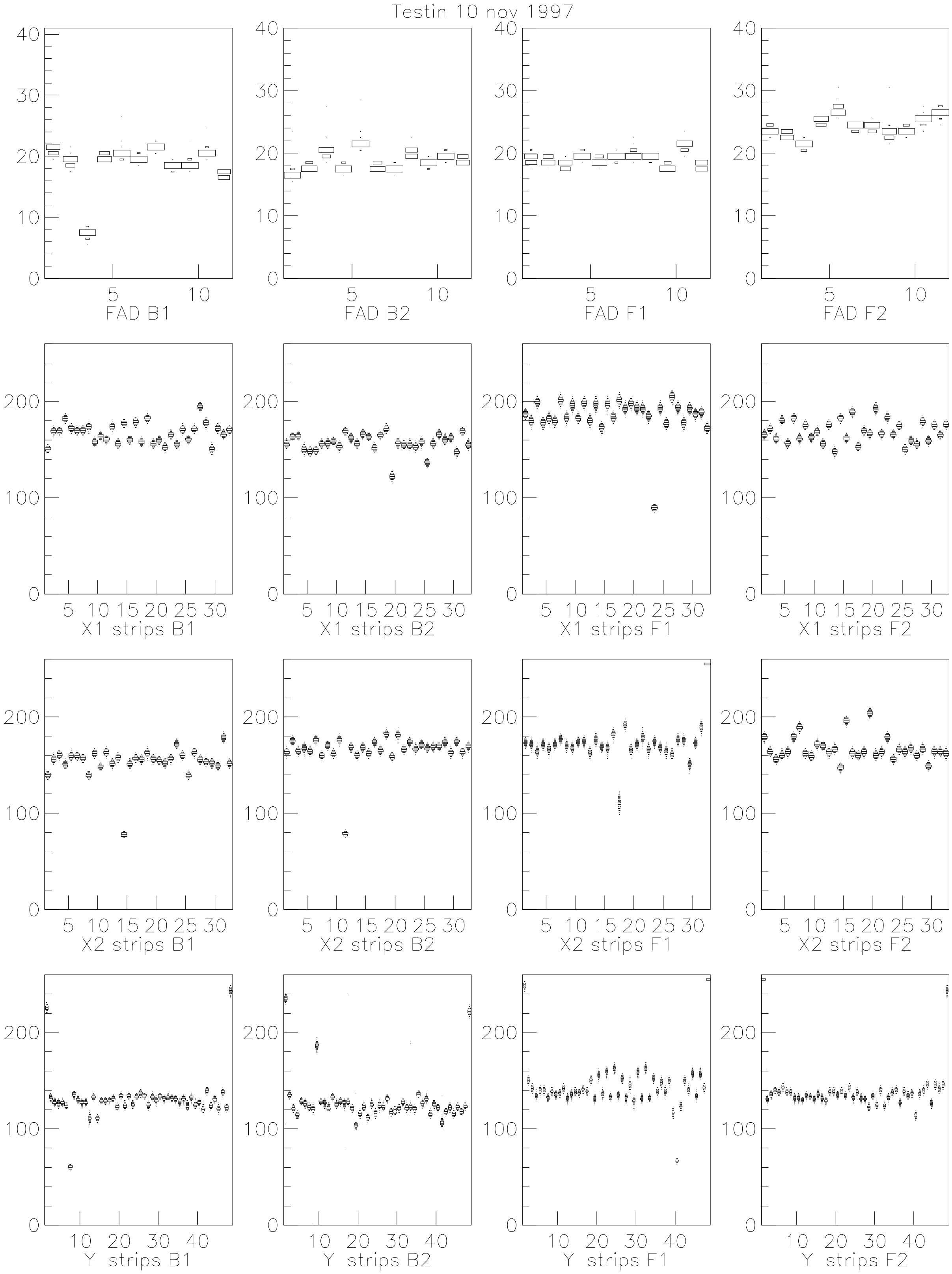

Figure 4: Pulse height in ADC units for TESTIN signal

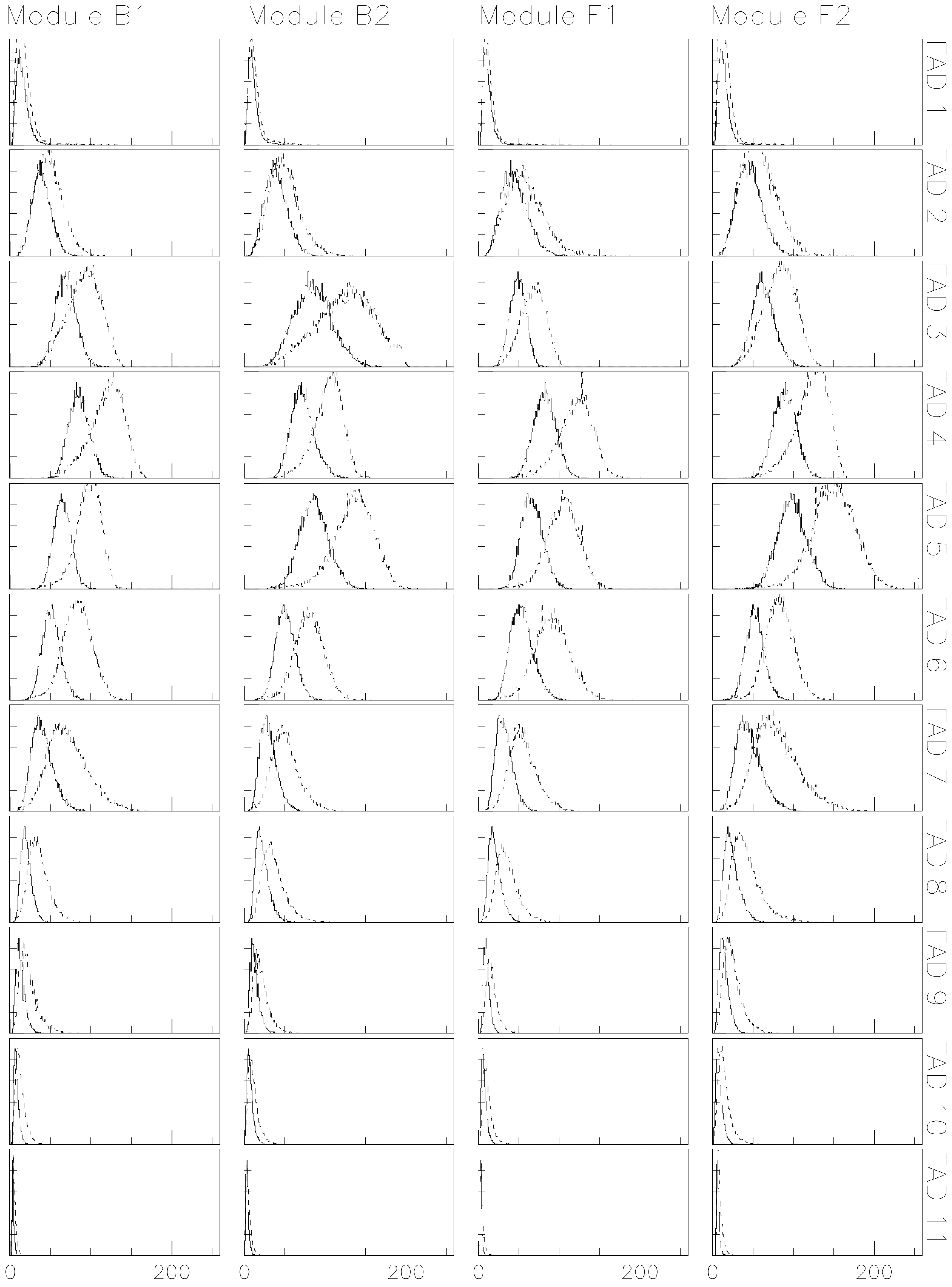

Figure 5: FAD pulse height distributions at 45 (solid line) and 68 (broken line) GeV

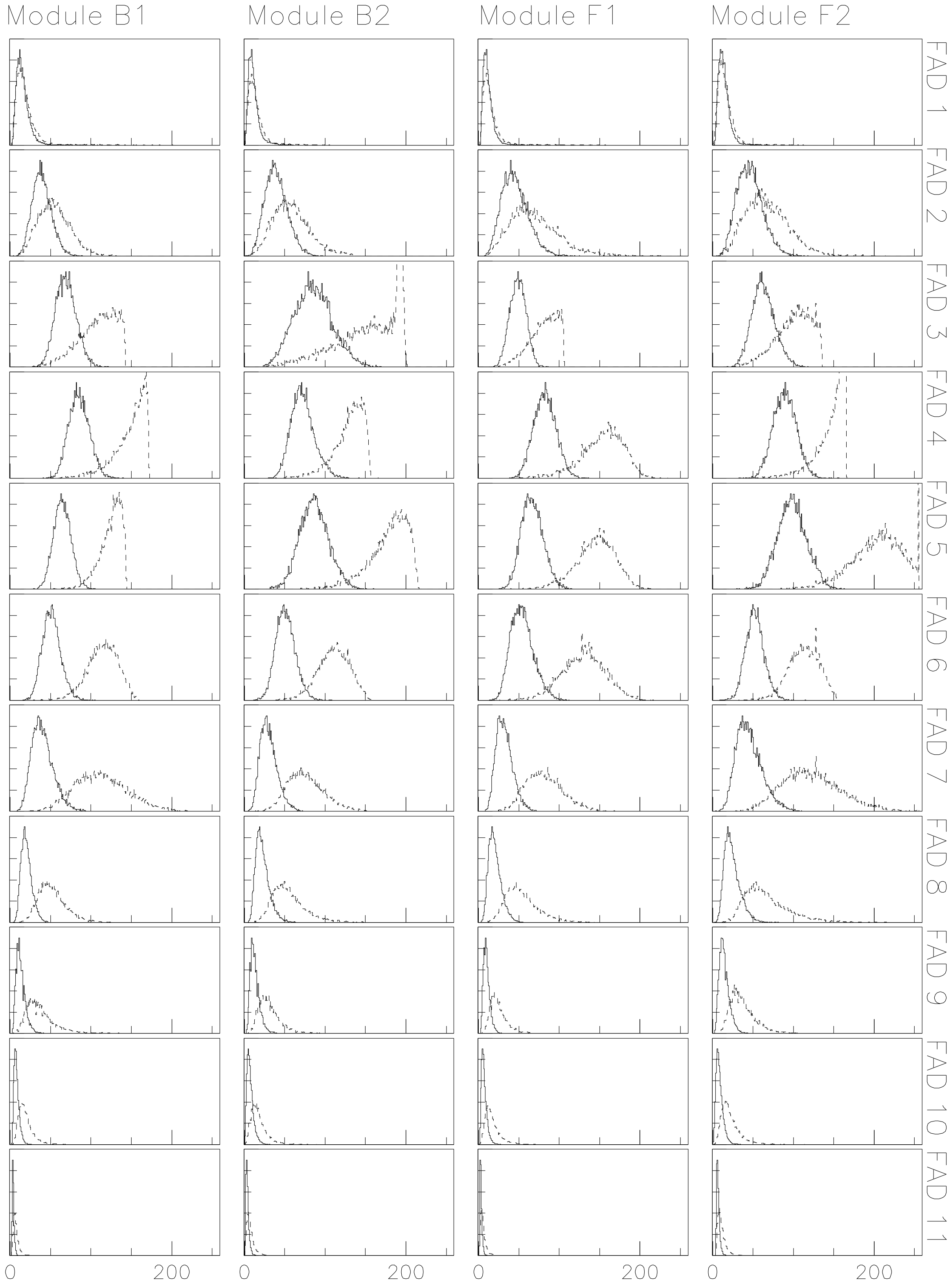

Figure 6: FAD pulse height distributions at 45 (solid line) and 91 (broken line) GeV

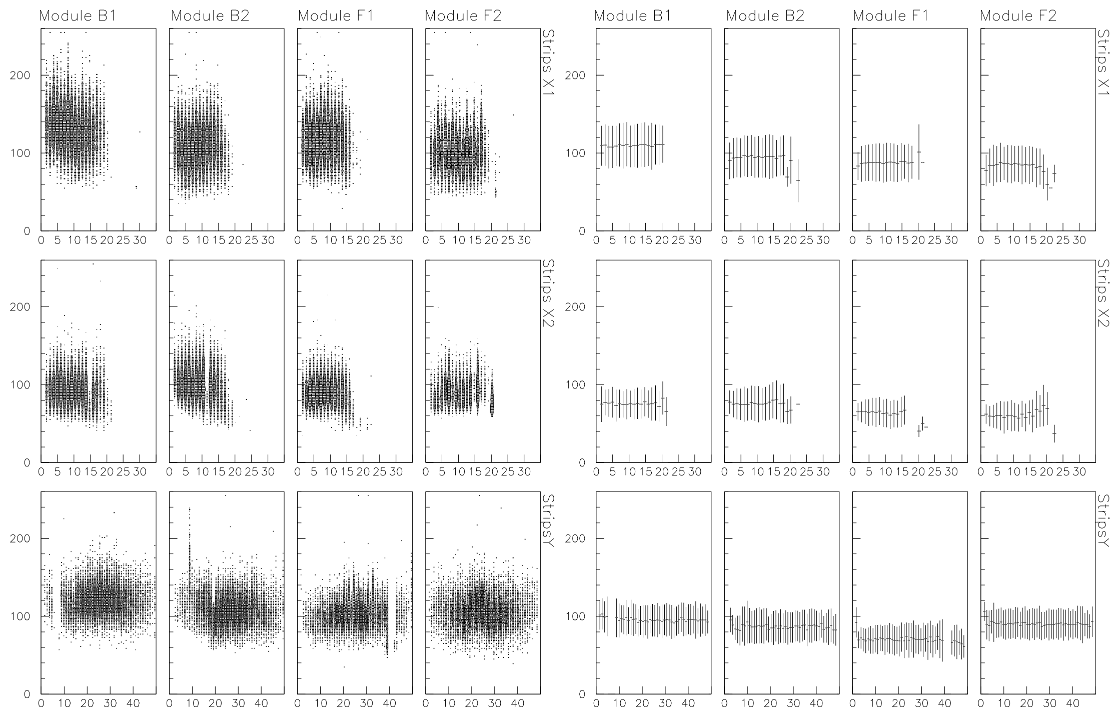

Figure 7: Pulse height distributions at 45 GeV of individual strips in x1,x2 and y strip planes, for the strip with maximum calibrated pulseheight. Left is the raw pulseheigth, to the right is the avarage pulseheight after calibration. The calibration is done at 45 GeV.

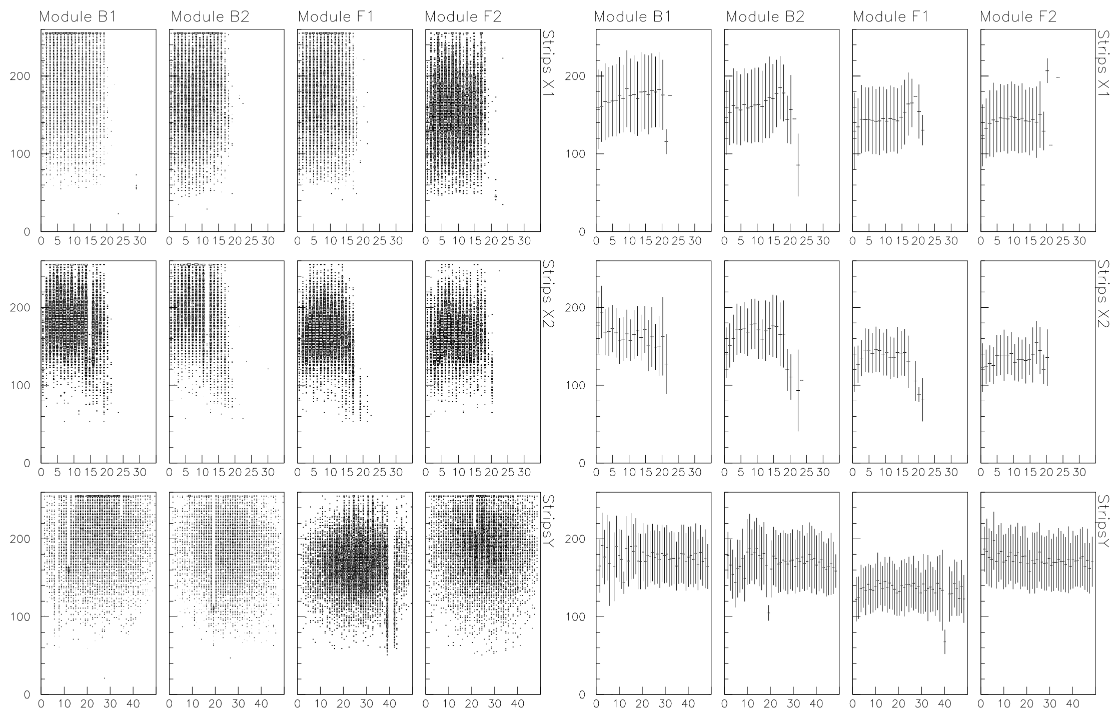

Figure 8: Pulse height distributions at 91 GeV of individual strips in x1,x2 and y strip planes, for the strip with maximum calibrated pulseheight. Left is the raw pulseheigth, to the right is the avarage pulseheight after calibration. The calibration is done at 45 GeV.

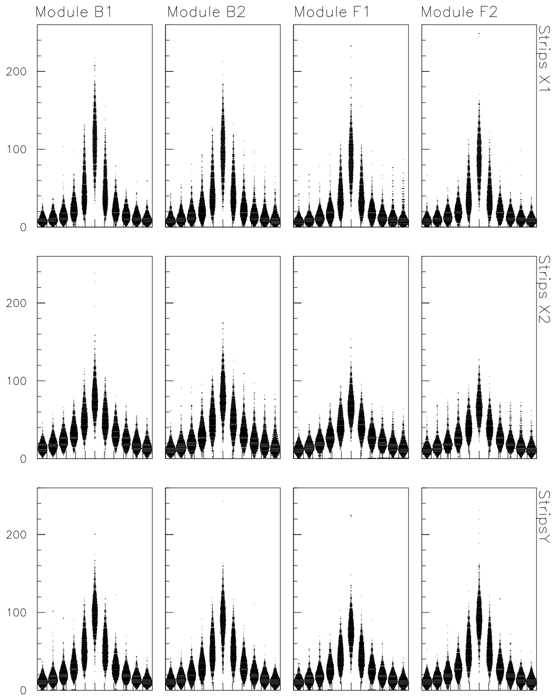

Figure 9: The shower profile for the different strips planes at 45 GeV. The strip with the maximum energy deposited is put in the middle.

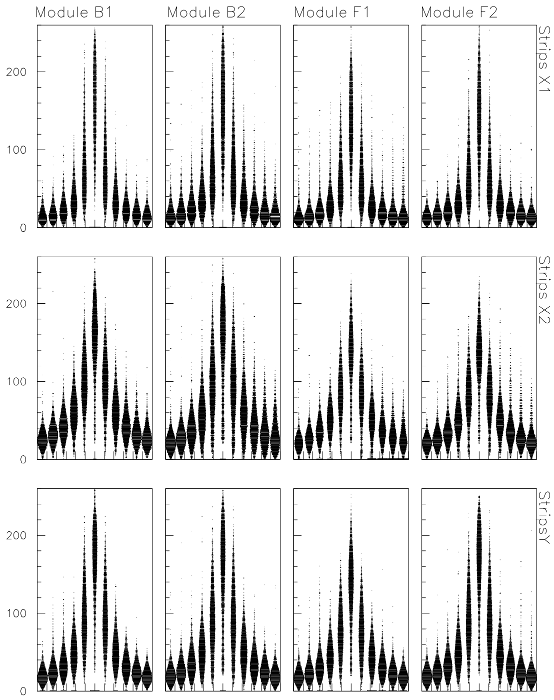

Figure 10: The shower profile for the different strips planes at 91 GeV. The strip with the maximum energy deposited is put in the middle.

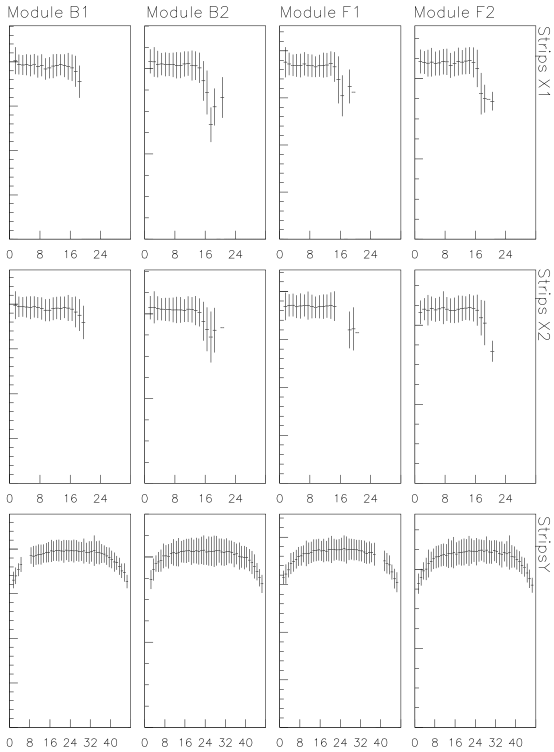

Figure 11: Total pulse height (arbitrary units) at 45 GeV for a module as a function of the reconstructed shower position in x1,x2, and y strip planes.

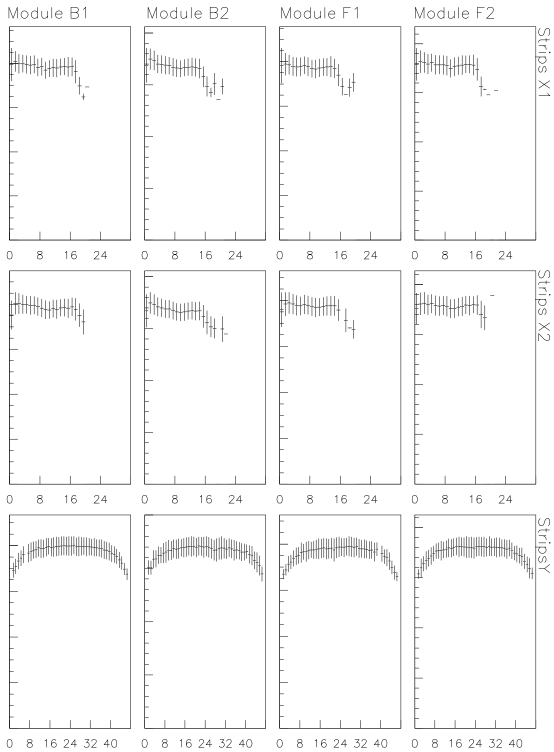

Figure 12: Total pulse height (arbitrary units) at 91 GeV for a module as a function of the reconstructed shower position in x1,x2, and y strip planes.

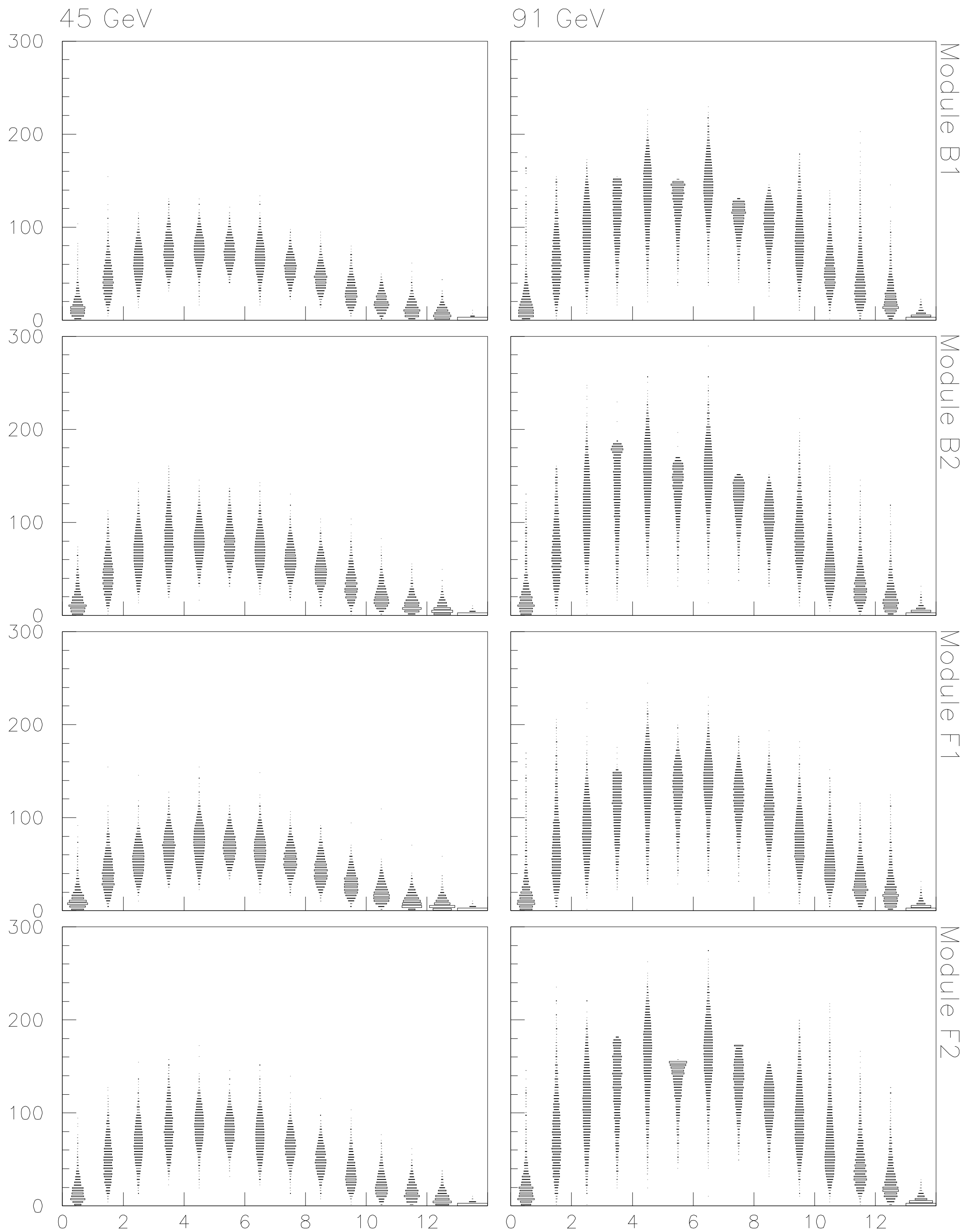

Figure 13: Shower profiles at 45 GeV (left) and 91 GeV (right). On the Y-axis is the calibrated ADC values, on the X-axis FAD/strip plane number. The strip planes are at positions 2,4, and 6.

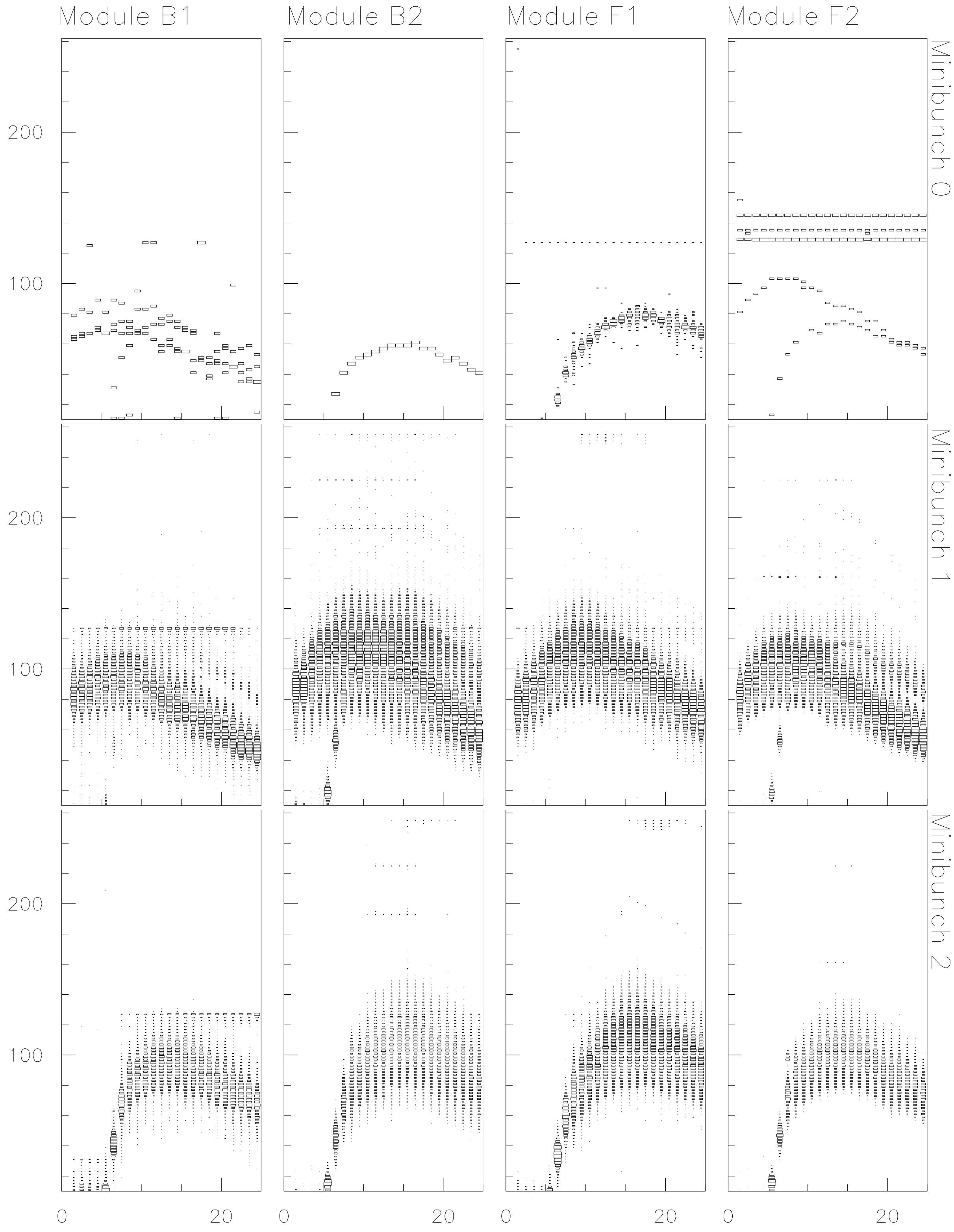

Figure 14: The analog trigger sum pulse shape at 45 GeV using the FADC on LURFB, and for different minibunch tags. Minibunch 0 are untagged events. On the y-axis is the FADC values, on the x-axis FADC sample number. The time inbetween FADC samples are 50 ns.

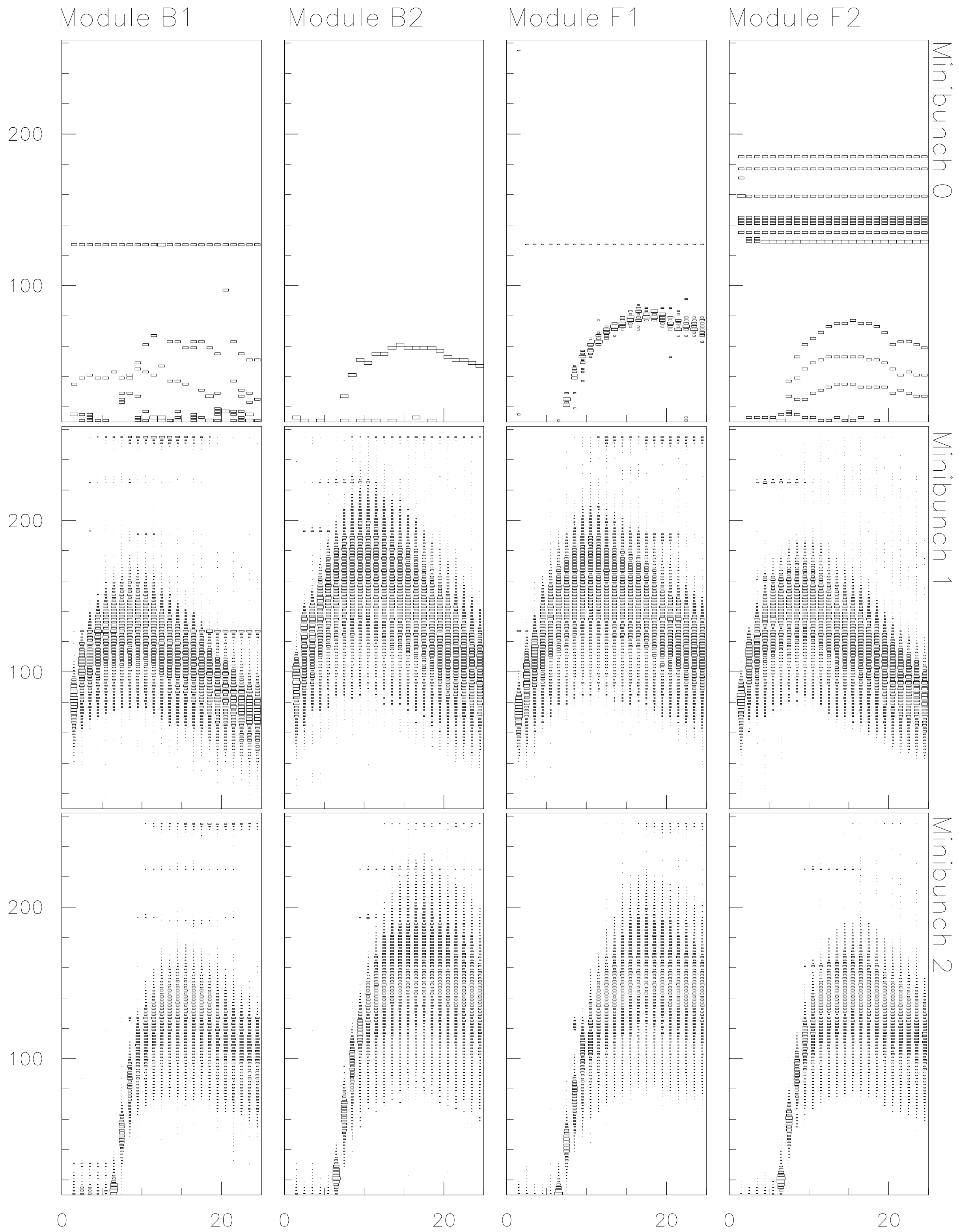

Figure 15: The analog trigger sum pulse shape at 68 GeV using the FADC on LURFB, and for different minibunch tags. Minibunch 0 are untagged events. On the y-axis is the FADC values, on the x-axis FADC sample number. The time inbetween FADC samples are 50 ns.

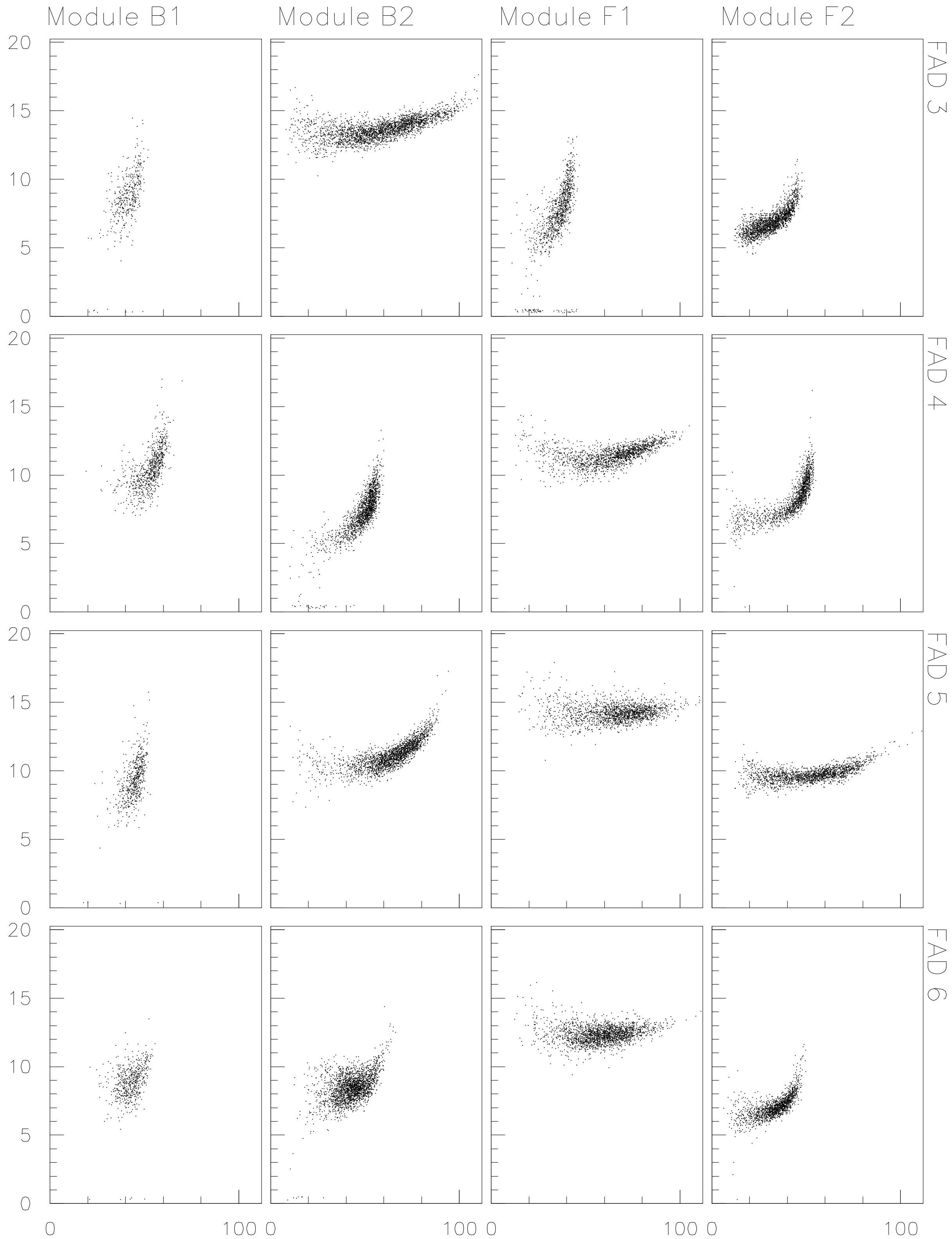

Figure 16: The peaking time of individual FAD signals relative the pulseheight at the peaking time. The time is units of FADC samples, i.e. 50ns per sample, and relative to the first FADC sample. The FADs shown are from top to bottom: 3,4,5, and 6, for each module.

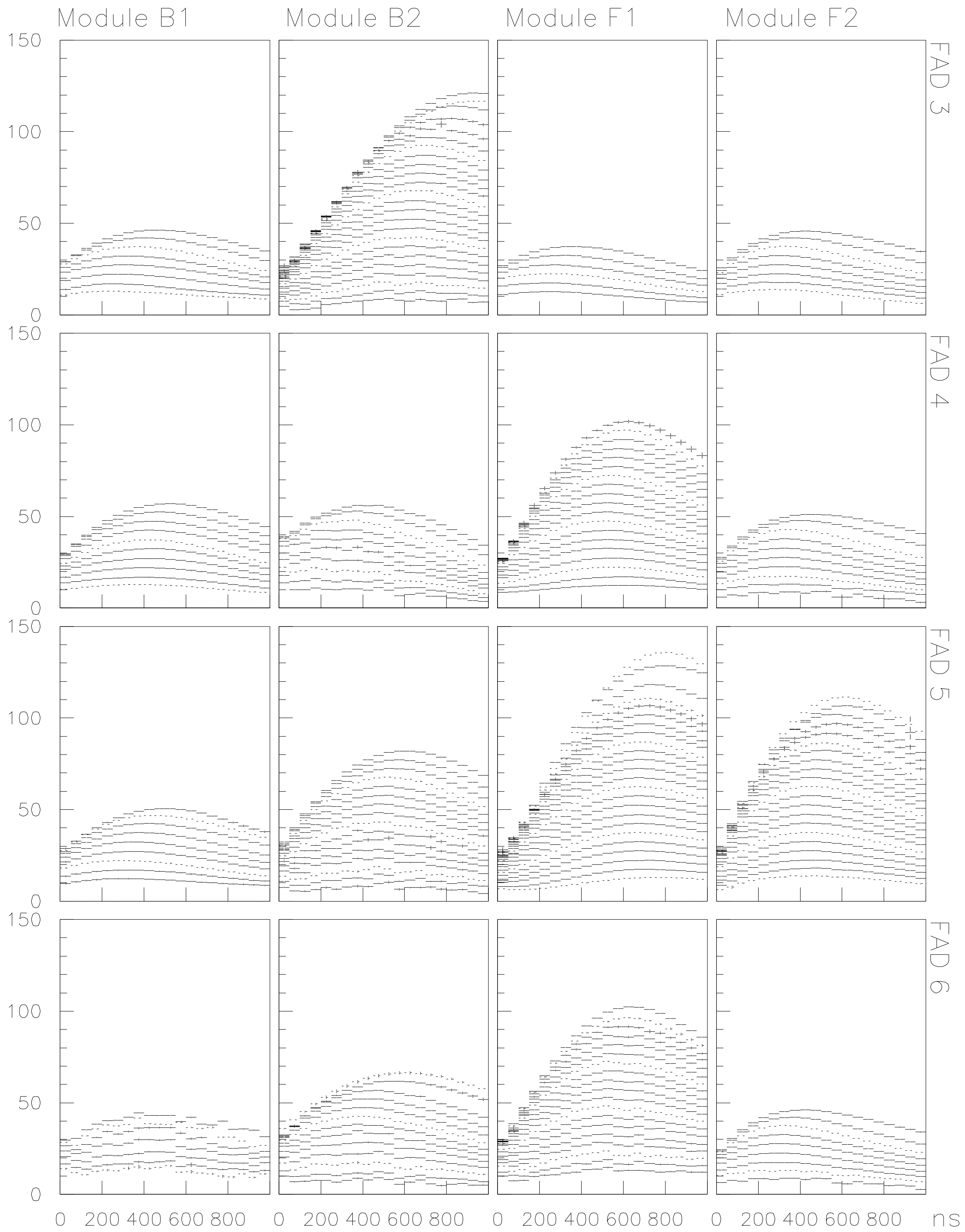

Figure 17: Examples av individual FAD signals for different pulseheights. Each line represents the average of events with the maximum pulse height in intervals of 5 FADC values.

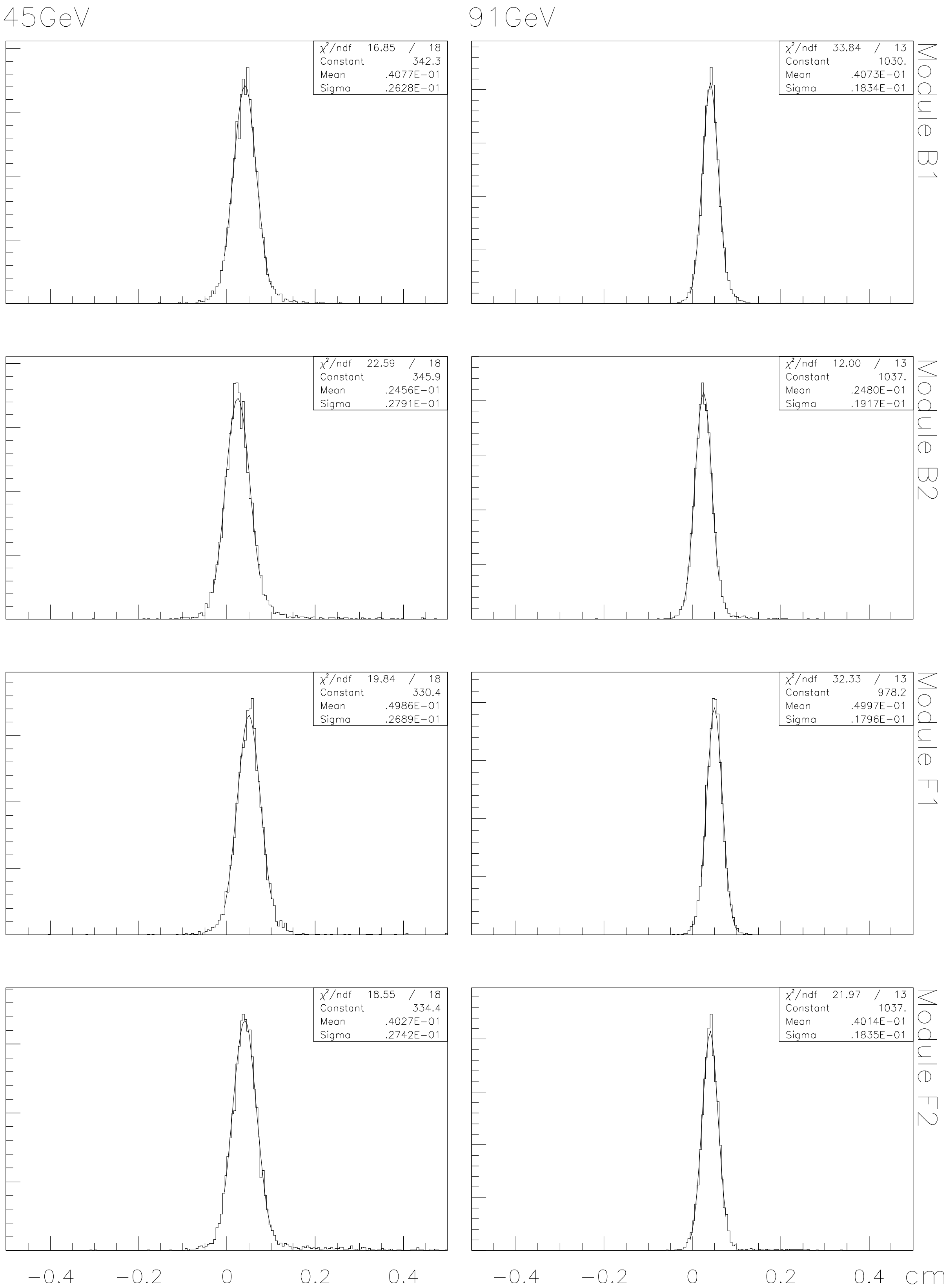

Figure 18: Difference between the reconstructed position in X2 and X1 strip planes at 45 GeV (left) and 91 GeV (right)

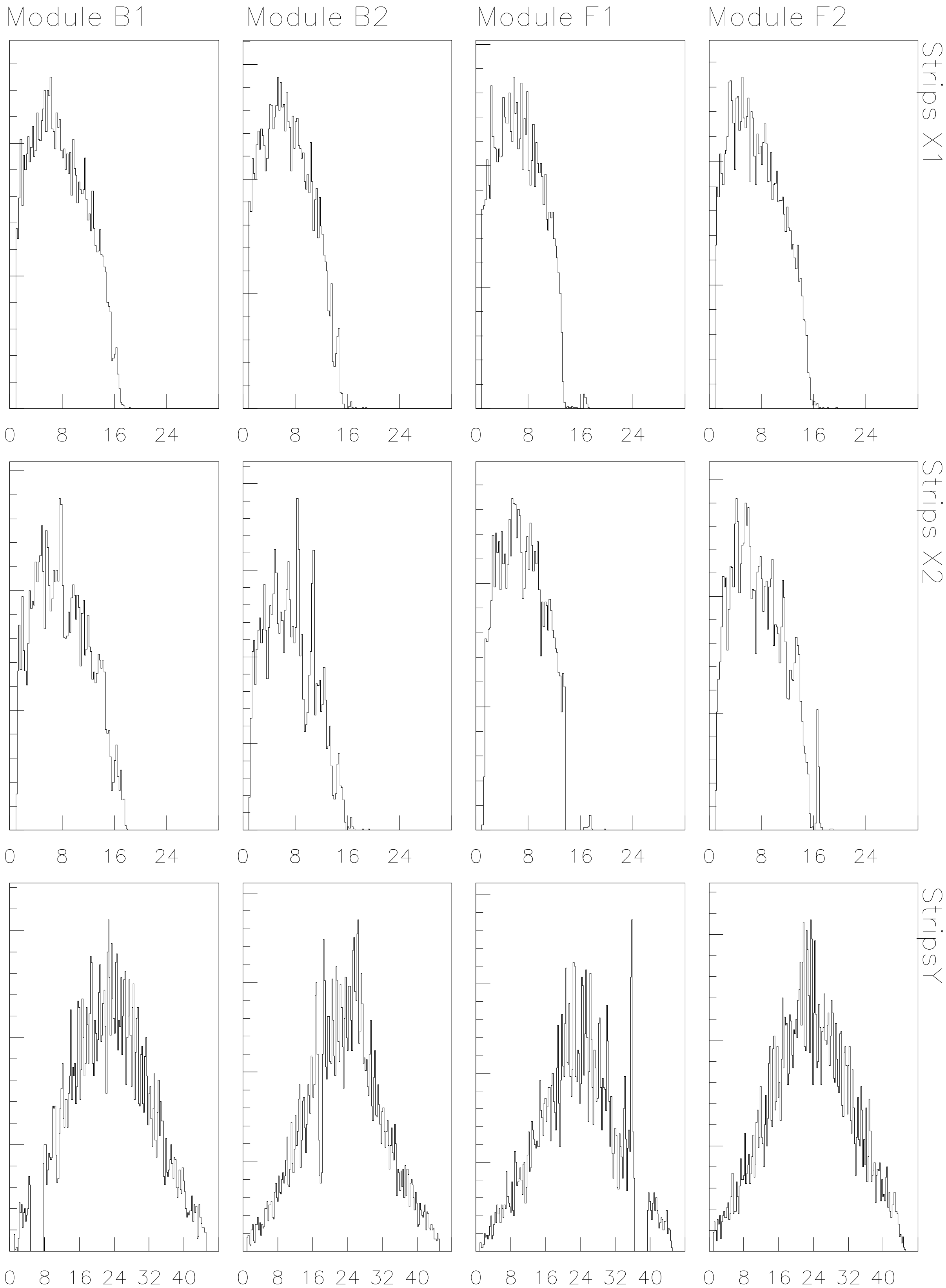

Figure 19: Reconstructed positions in x1, x2, and y for bhabha events at 91 GeV.

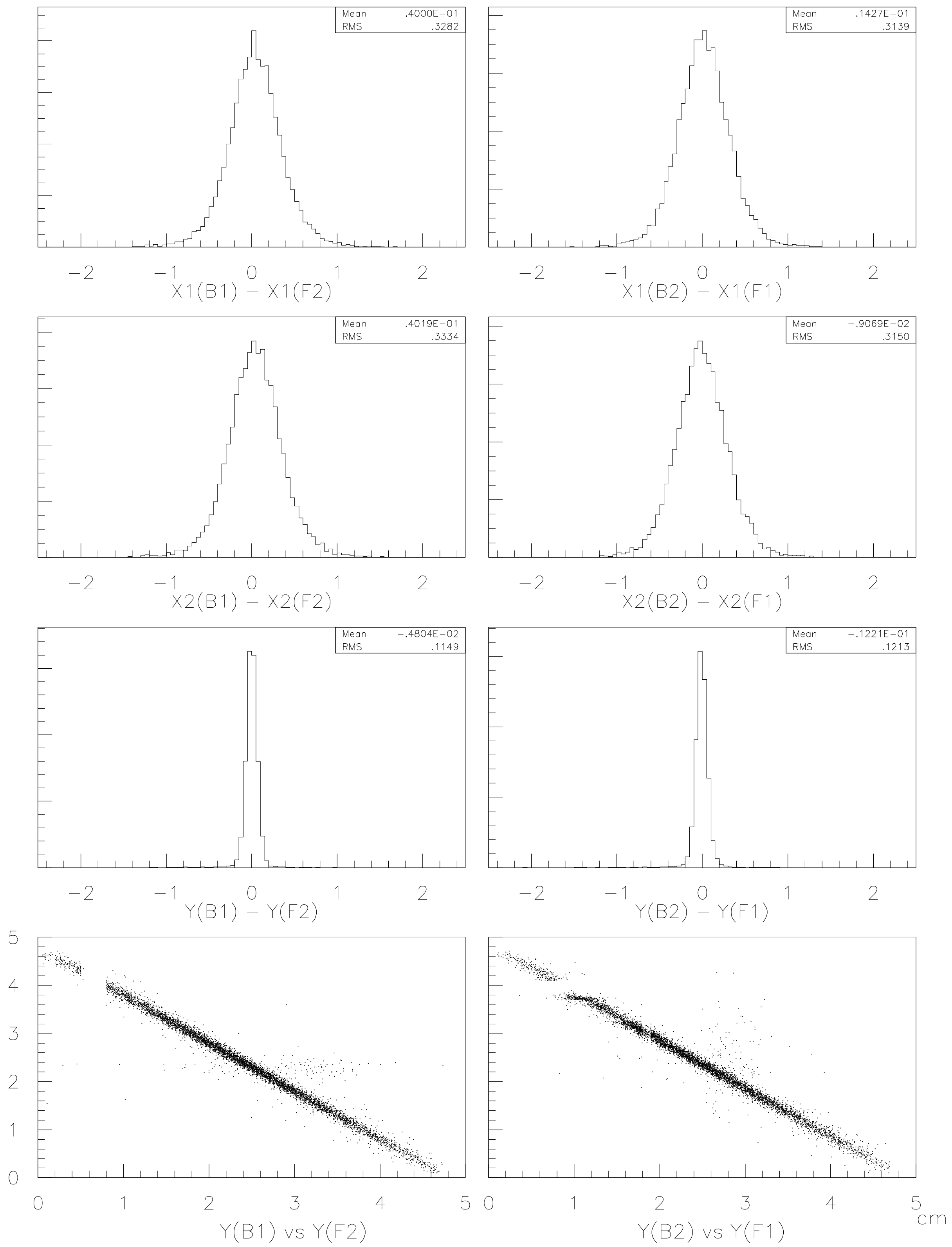

Figure 20: Colinearity between diagonal modules for bhabha events, events outside the diagonal band is background

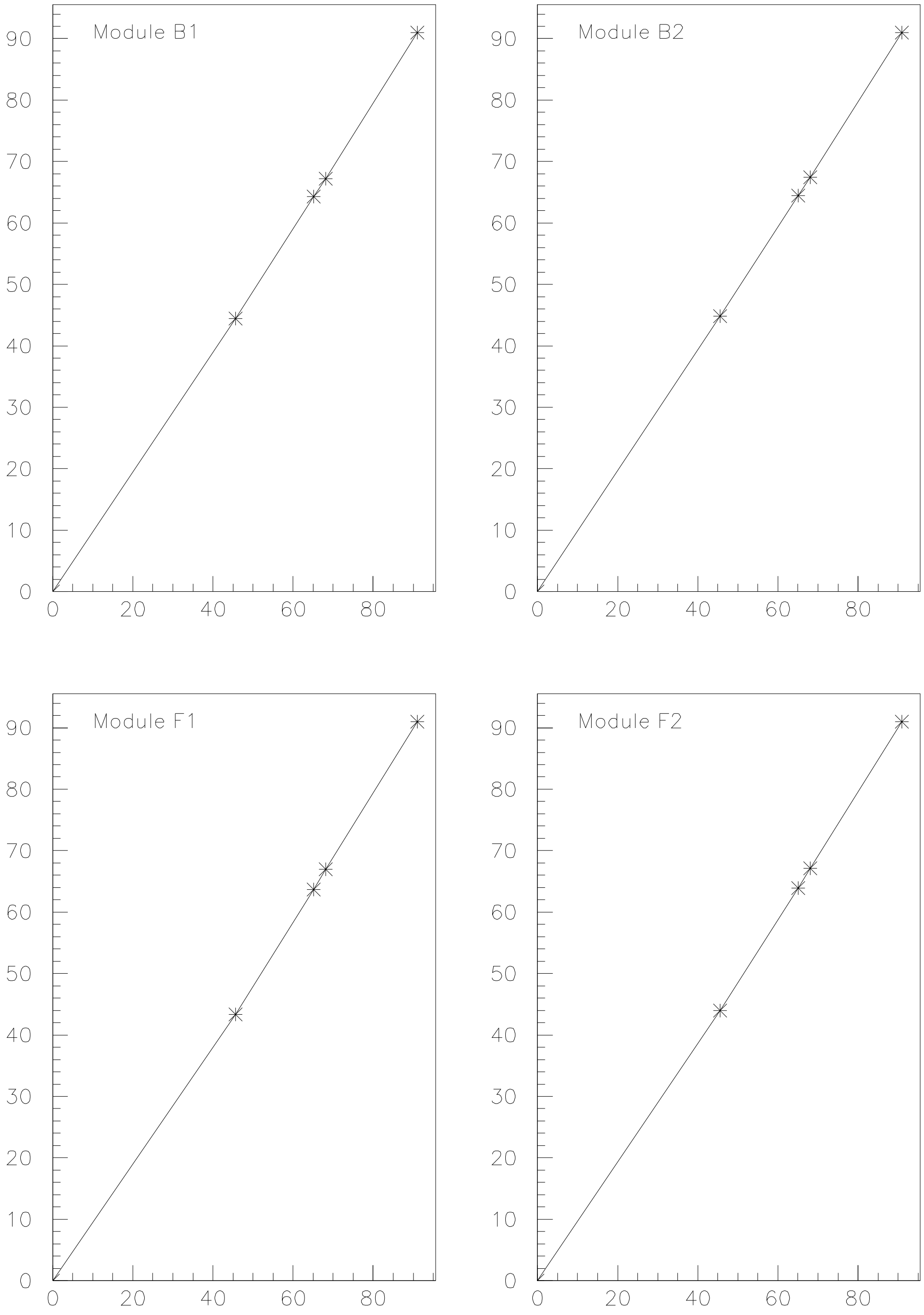

Figure 21: The energy response when using strips instead of FAD palens 3,4,and 5. The line is a guide to the eye.

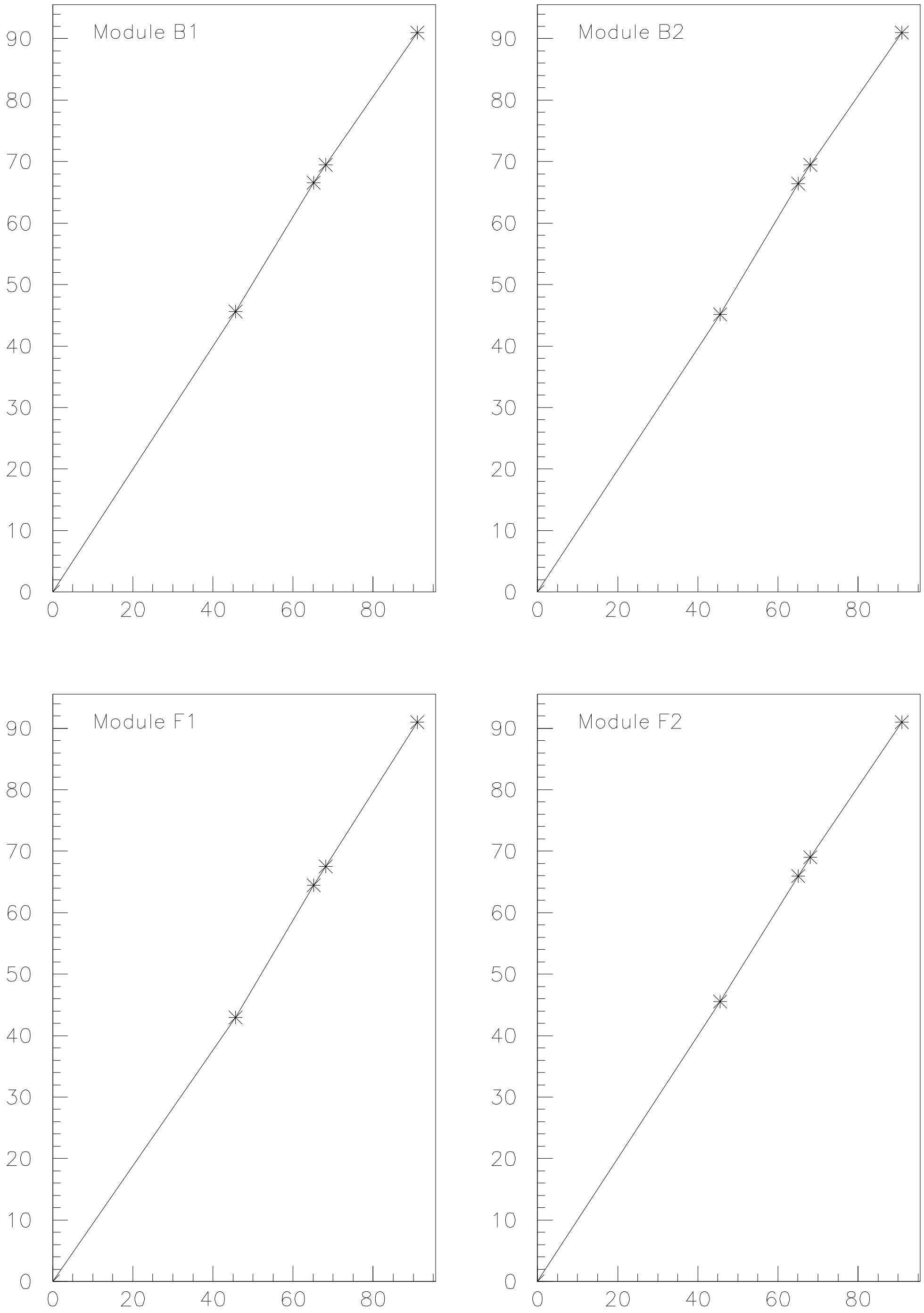

Figure 22: The energy response when using FAD planes 3,4,and 5.The line is a guide to the eye.

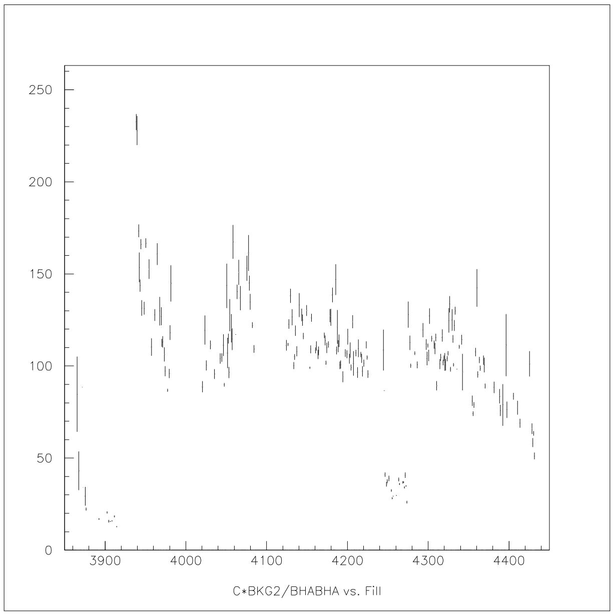

Figure 23: Background 1997 vs fill number

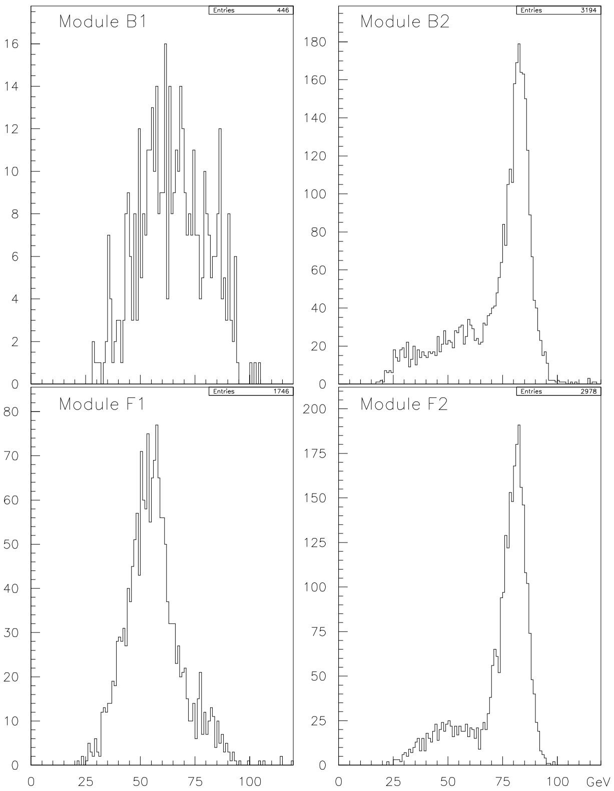

Figure 24: Energy distribution at 91 GeV of events with energy deposited in one module, and nothing in the diagonal module.

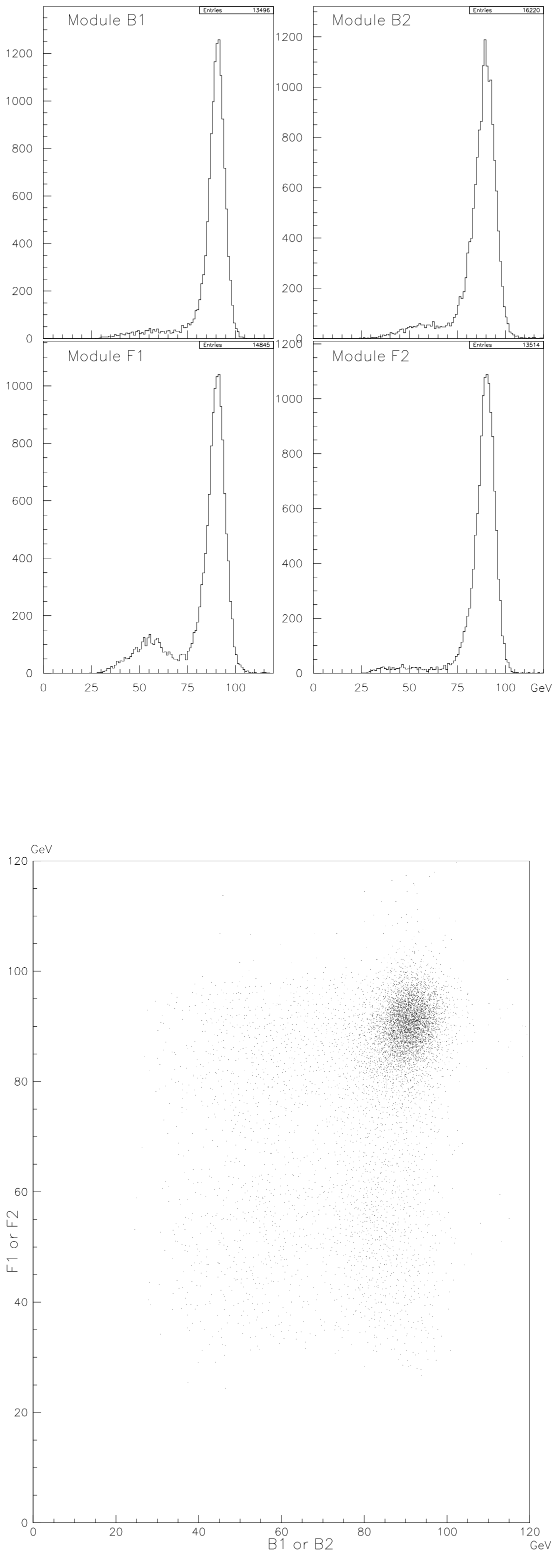

Figure 25: Total reconstructed energies at 91 GeV. The bottom figure shows a scatter plot between diagonal modules.